ELSEVIER

Catalysis Today 41 (1998) 207–219

CATALYSIS TODAY

Surface area and pore texture of catalysts

G. Leofanti[a,*], M. Padovan[b], G. Tozzola[c], B. Venturelli[c]

[a] *Consultant, Via Firenze 43, 20010 Canegrate, Italy*
[b] *Consultant, Via Villa Mirabello 1, Milano, Italy*
[c] *Enichem S.p.A., Enichem Base Research Center, Via G. Fauser 4, 28100 Novara, Italy*

Abstract

The origin, the classification and the effect on catalytic performance of pore texture of heterogeneous catalysts are briefly examined. The techniques and the methods suitable for the determination of related properties (surface area, pore volume and pore size distribution) are reviewed. Particular attention is paid to the most widely used ones: vapour adsorption at low temperature, mercury porosimetry, incipient wetness impregnation and picnometry. Advantages, disadvantages and applicability of each method to different pore textures are pointed out. The best choice of a group of methods, allowing a complete characterization of catalysts, is proposed.

Keywords: Surface area; Pore volume; Pore size; Nitrogen adsorption; Hg porosimetry

1. Introduction

Most heterogeneous catalysts are porous solids.

The pore texture arises from the preparation methods of these solids [1–3]:

1. precipitation from a solution originates precursor particles that agglomerate and form a porous structure;
2. hydrothermal crystallization produces zeolites or other crystalline microporous compounds, where the peculiar arrangement of the "building units" generates intracrystalline cavities of molecular size;
3. elimination of volatile materials during thermal treatments (burning, evaporation) produces cavities as the result of both solid rearrangement and exit way of the removed material;
4. selective dissolution of some components can produce pores;
5. different shaping procedures, employed to obtain the catalyst suitable for industrial reactors (tableting, extrusion, spray drying), give rise to stable aggregates of particles that containing a porous structure correspondent to intraparticle voids.

In such a way a typical catalyst contains one or more groups of pores, whose size and volume depend on preparation method.

The pores are classified in different classes depending on their size [1–5]:

1. micropores (size <2 nm), ultramicropores (size <0.7 nm),
2. mesopores (2 nm <size<50 nm),
3. macropores (size >50 nm).

Pores can have a regular or, more commonly, an irregular shape. The most similar geometric form is

---

*Corresponding author.

0920-5861/98/$32.00 © 1998 Elsevier Science B.V. All rights reserved.
PII S0920-5861(98)00050-9

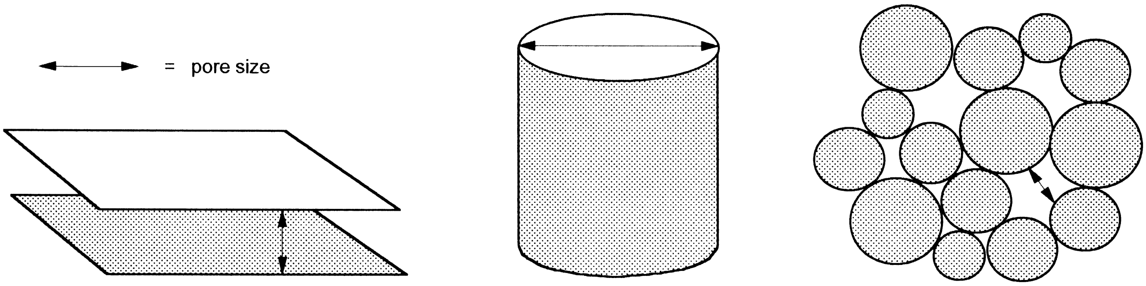

Fig. 1. Common models of pores.

used to represent pore shape: cylinders (in some oxides like alumina and magnesia), slits (in activated carbons and clays) and voids between connected solid spheres (in silica and many solids obtained from gels), as shown in Fig. 1. Cylinders (size=diameter) and slits (size=distance between walls) are the most widely used models being simple to handle.

These models assume that each pore has a uniform size along the length, but very often they are ink-bottle shaped (pore body larger than pore mouth) or funnel shaped (the contrary): the physical meaning of the term pore size depends on the method used to investigate the porous texture. Last, catalyst granules contain generally pores of different size, so we must consider the pore size distribution, that is the pore volume against pore size (Fig. 2).

Pores can be closed (not accessible from the external), blind (open at only one end), or through (open at both ends). Each pore can be isolated or, more frequently, connected to other pores to form a porous network (Fig. 2)

The irregular shape of pores and their connectivity cause a molecule to cover a distance greater than the granule size when pass through a catalyst granule. The ratio between distance covered and granule size is sometimes called tortuosity factor.

Porous solids have a total surface much higher than that corresponding to the external one, because of contribution of pore walls. The most common catalysts have a specific surface area between 1 and 1000 $m^2\ g^{-1}$, while their external surface area is in the range 0.01–10 $m^2\ g^{-1}$.

Knowledge of morphological parameters allows understanding of catalyst evolution during preparation procedure and gives a feedback useful for modifying the method to obtain the desired results.

The same way, knowledge of morphological parameters is useful to comprehend the catalytic behaviour in the reaction environment. On one hand the catalytic process takes place on the surface of the catalyst, then its area strongly affects the catalytic activity. On the other hand, to reach the surface, the reagent molecules

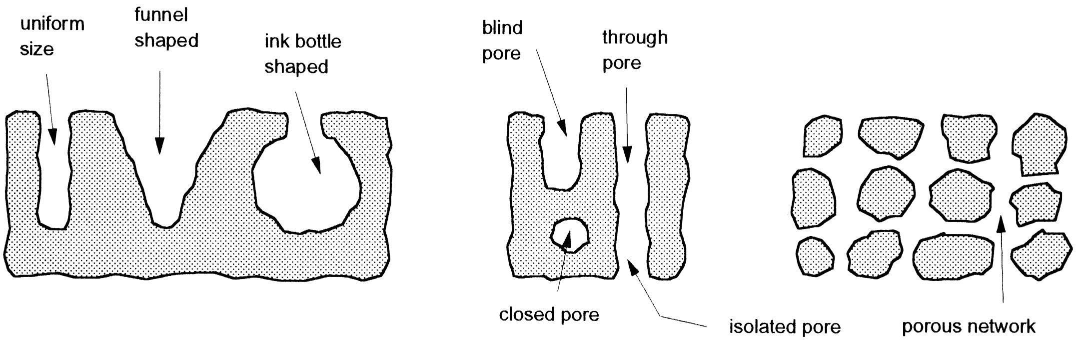

Fig. 2. Types of pores.

must run across the porous system, as well as the reaction products have to leave the catalyst. Mass transfer process inside the granules depends on pore size (bulk diffusion in macropores, Knudsen diffusion in mesopores and molecular diffusion in micropores) and tortuosity factor.

Also deactivation phenomena are greatly affected by pore size. Carbonceous deposition blocking of micro and mesopore mouths and covering meso and macropore walls are typical examples.

Several information on the above summarized topics can be found in [5–10].

Morphological characteristics of interest are surface area, pore volume, area and pore size distributions.

There are a variety of techniques to determine these characteristics. The right choice depends on type of pores and on the use we want to do of such data.

In this paper the different methods are briefly discussed, according to the following criteria:

1. the space reserved to theory has been reduced to the minimum indispensable, being the information easily available in the literature,
2. the instrumentation is not described because nowadays quite only automatized commercial instruments are used,
3. the problems usually encountered in the practice, the obtainable information and the limits of different methods are emphasized,
4. when different approaches to determine the same characteristic can be used, the preferable techniques are indicated on the basis of our experience.

The readers interested to go deep into one or more topic, schematically presented in this introductory paper, are addressed to the wide set of enclosed references.

2. Techniques and methods for determination of morphological characteristics: an overview

The most important methods and techniques for quantitative morphological characterization are reported in Table 1

In the following sections techniques and methods are briefly discussed. The space devoted to a single topic is determined by the importance we attribute to the technique or to the method on the basis of our experience.

3. Nitrogen adsorption at 77 K (surface area, pore volume and size distribution)

Nitrogen adsorption at boiling temperature (77 K) represents the most widely used technique to determine catalyst surface area and to characterize its porous texture. Starting point is the determination of the adsorption isotherm, that is the nitrogen adsorbed volume against its relative pressure.

Isotherm shape depends on the solid porous texture. According to IUPAC classification six types can be distinguished, but only four are usually found in catalyst characterization ([3,6–8]; Fig. 3).

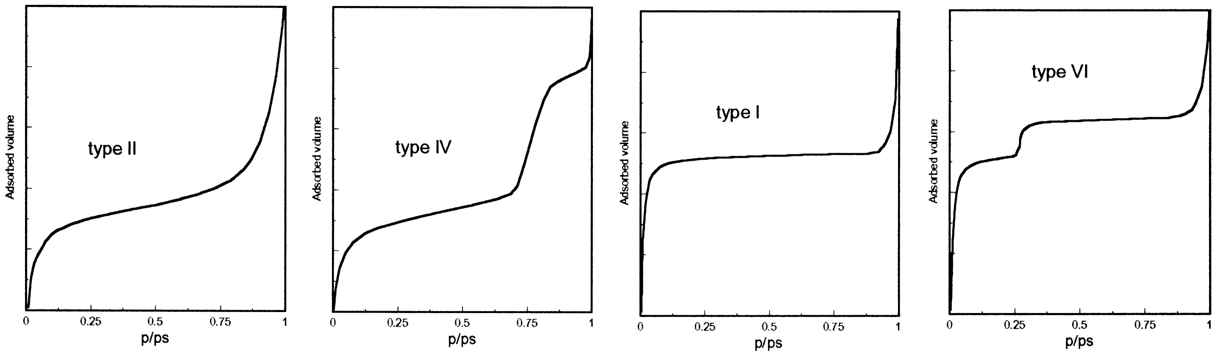

Fig. 3. The four types of adsorption isotherm usually found by nitrogen adsorption.

Table 1
Techniques and methods for determination of morphology characterization

Technique	Method	Information	Micropores	Mesopores	Macropores
N_2 adsorption at 77 K	BET	surface		X	X
	t-plot	area		X	X
	a_s-plot				
Kr, Ar, He, ads. at low temp	BET			X	X
N_2 adsorption at 77 K	BJH	surface area=		X	
	DFT	*f*(pore size)	X	X	X
N_2 adsorption at 77 K	*t*-plot	pore	X	X	
	a_s-plot	volume	X	X	
	DR		X		
	MP		X		
	korvath–Kavazoe		X		
	DFT		X	X	
	BJH			X	
	Gurvitsch		X	X	
Kr, Ar, He ads. at low temp.	Various methods		X	X	X
Hg porosimetry	Washburn		X	X	X
Incipient wetness			X	X	
From true and particle density			X	X	X
N_2 adsorption at 77 K	MP	pore volume=	X		
	Horvath–Kavazoe	*f*(pore size)	X		
	DFT		X		
	BJH			X	
Hg porosimetry	Washburn			X	X
All techniques	Calculated from V_n and A_s	average pore size	X	X	X
Permeametry			X	X	X
Counterdiffusion			X	X	X

(1) *Macroporous solids* (*type* II). At low relative pressure formation of a monolayer of adsorbed molecules is the prevailing process, while at high relative pressure a multilayer adsorption takes place: the adsorbate thickness progressively increases until condensation pressure has been reached. The pressure of first monolayer formation is lower if the interaction between adsorbate and adsorbent is stronger, but monolayer and multilayer formation processes are always overlapped.

(2) *Mesoporous solids* (*type* IV). At low relative pressures the process does not differ from what happens in macroporous solids. At high relative pressures the adsorption in mesopores leads to multilayer formation until, at a pressure dependent on Kelvin-type rules (larger mesopore=higher pressure), condensation takes place, giving a sharp adsorption volume increase. As mesopores are filled adsorption continues on the low external surface. Most oxides used as carriers and most catalysts belong to this class of solids.

(3) *Microporous solids* (*type* I). The adsorption takes place also at very low relative pressures because of strong interaction between pore walls and adsorbate. The completion of filling require often a bit higher pressure favoured by interaction between adsorbed molecules. In this case pore filling takes place without capillary condensation in the low relative pressure region (<0.3). This way the process is indistinguishable from the monolayer formation process. Once micropores are filled, the adsorption continues on the external surface, following the behaviour described for macro or mesoporous solids. Typical examples of microporous solids are active carbons, zeolites and zeolite-like crystalline solids.

(4) *Uniform ultramicroporous solids* (*type* VI). The pressure at which adsorption takes place depends on

surface–adsorbate interaction, so, if the solid is energetically uniform, the whole process happens at a well-defined pressure. If the surface contains few groups of energetically uniform sites, a stepped isotherm must be expected, each step corresponding to the adsorption on one group of sites. Since all the catalyst surfaces are widely heterogeneous this behaviour has never been observed. Stepped-like isotherms have been obtained only in the case of well crystallized zeolites like X (one step corresponding to cavities filling) or silicalite (two steps, corresponding, respectively, to channel filling and to an adsorbent–adsorbate transition).

The adsorbate desorption, after saturation is reached, is the opposite of the adsorption, but evaporation from mesopores usually takes place at a pressure lower than that of capillary condensation giving an hysteresis. This is due to pore shape and four types of hystereses have been recognized, according to IUPAC classification [2,3,11]; Fig. 4.

(1) *Types* H1 *and* H2 *hystereses.* These types are characteristic of solids consisting of particles crossed by nearly cylindrical channels or made by aggregates (consolidated) or agglomerates (unconsolidated) of spheroidal particles. In both cases pores can have uniform size and shape (type H1) or nonuniform size or shape (type H2). Hysteresis is usually attributed to different size of pore mouth and pore body (this is the case of ink-bottle shaped pores) or to a different behaviour in adsorption and desorption in near cylindrical through pores. In ink-bottle pores the condensation takes place in each section at the relative pressure provided by Kelvin law (the liquid formed at low pressure in the pore mouth supplies the vapour for adsorption and condensation in the large pore body), but the evaporation from the pore body cannot occur until the pore mouth remains filled. In the case of cylindrical pores the meniscus is cylindrical during condensation and hemispherical during evaporation. Most common mesoporous carrier and catalysts belong to this class [2,3,12,13]

(2) *Types* H3 *and* H4 *hystereses.* These hystereses are usually found on solids consisting of aggregates or agglomerates of particles forming slit shaped pores (plates or edged particles like cubes), with uniform (type H4) or nonuniform (type H3) size and/or shape. Hysteresis is usually due to a different behaviour in adsorption and desorption. For example in pore formed by parallel plates the meniscus is flat (radius$=\infty$) during adsorption (condensation does not take place at any relative pressure) and cylindrical (radius=half the distance between plates) during desorption. Typical examples of this class are active carbons and zeolites [2,3,14,15].

(3) *No hysteresis.* This is the case of blind cylindrical, cone-shaped and wedge-shaped pores. Since catalyst pores are usually irregular we can observe only solids with very reduced hysteresis loop [3].

The low pressure closure of the hysteresis loop takes place at a relative pressure of 0.42 for nitrogen, independently of the adsorbent and of the pore size distribution and is related to the liquid adsorbate properties, as shown in Section 3.8.

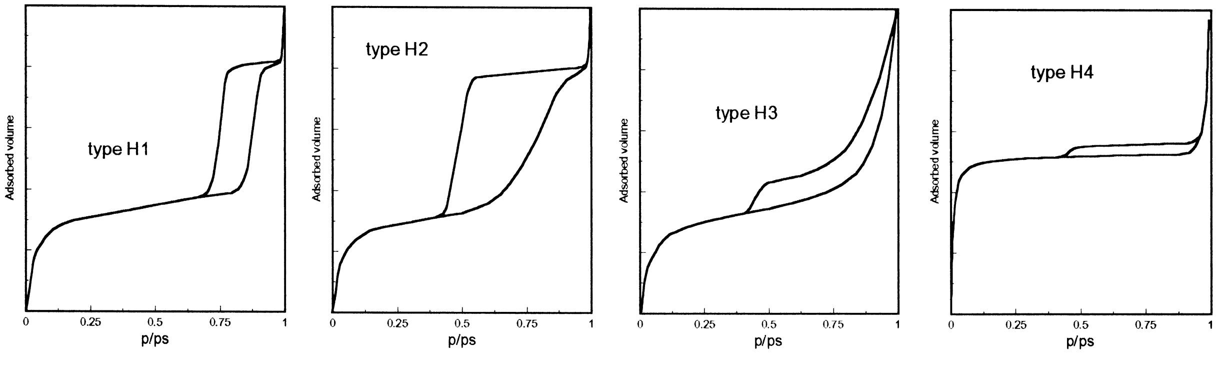

Fig. 4. The four hysteresis shapes of adsorption isotherm usually found by nitrogen adsorption.

3.1. BET method (surface area)

The model, developed by Brunauer, Emmet and Teller in 1940s [16,17], still remains the most diffuse tool to determine the monolayer volume (V_m) of the adsorbate, and then the surface area (A_s) of solids by the equation [3]:

$$A_s = (V_m/22414)N_a\sigma,$$

where N_a is Avogadro number and σ the area covered by one nitrogen molecule. The σ value generally accepted is 0.162 nm^2 [3,18–20].

V_m can be estimated by the three parameters BET equation, developed assuming that [3,21,22]:

1. the heat of adsorption of first monolayer is constant (the surface is uniform as concerns the adsorption),
2. the lateral interaction of adsorbed molecules is negligible,
3. the adsorbed molecules can act as new adsorption surface and the process can repeat itself,
4. the heat of adsorption of all monolayers but the first is equal to the heat of condensation.

According to the model the adsorbed volume (V_{ads}) depends on relative pressure (p/p_s), V_m, a parameter (c) related to heat of adsorption and liquefaction (high c=strong adsorbate–adsorbent interaction), a parameter (n) formally related to the mean number of layer that can be formed on the solid. The equation (three parameters BET equation) has the form:

$$V_{ads} = V_m \frac{cp/p_s}{1-p/p_s} \frac{1-(n+1)(p/p_s)^n + n(p/p_s)^{n+1}}{1+(c-1)(p/p_s) - c(p/p_s)^{n+1}}.$$

If $n \rightarrow \infty$, the equation assumes the following form, known as two parameters BET equation:

$$V_{ads} = V_m \frac{cp/p_s}{(1-p/p_s)(1+(c-1)p/p_s)}.$$

Practically this equation is suitable for n>6 (macroporous and larger mesoporous solids): in this range the differences between the two forms of BET equation do not exceed the experimental error. For $n \leq 6$ the two parameters equation gives values of surface area lower (up to 20%) than the three parameters equation [3,21,23].

BET model has been submitted to many criticisms, because real surfaces do not follow the assumption of the model (see for example [3,21,24–27]). Nevertheless in the range of relative pressure 0.05–0.35 it is capable to interpolate the experimental data for most solids, giving surface area values near to the mark. Nowadays BET method is the most widely used to determine surface area of solids and it can be regarded as a reference method.

The main lack of applicability is the case of microporous solids: in this case the monolayer volume computed by BET equation corresponds to the micropore volume plus the monolayer volume on the surface external to micropores [2–4].

3.2. t-plot method (surface area, micropore and mesopore volume)

The method, developed by DeBoer and coworkers in 1965 [28], is based on the observation that, for a variety of macroporous solids, the adsorbed volume

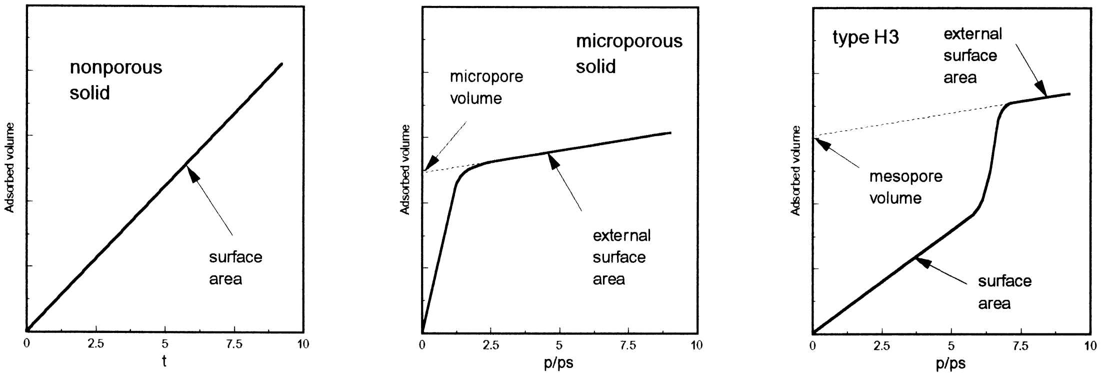

Fig. 5. The t-plot shapes of adsoption isotherm usually found by nitrogen adsorption

for unit surface (i.e. the statistical thickness t of the adsorbed layer) against pressure follows a single curve independent of the solid [3,29,30]. Then, by plotting V_{ads} on a given macroporous solid against t (the so called t-plot) a straight line passing through the origin of axes is obtained (Fig. 5). Its slope m is directly proportional to the surface area A_{s} of the solid:

$$A_{\mathrm{s}} = (m/22414)t_{\mathrm{m}}N_a\sigma.$$

If micropores are present [3,4,31–33] as they are progressively filled, the adsorption surface decreases and then decreases the slope of the t-curve until, after the complete filling, a straight line with a slope correspondent to the surface area external to micropores has to be expected. If extrapolated to t=0, this line gives a positive intercept correspondent to the adsorbed volume necessary to fill micropores. The total surface area cannot be measured in the presence of ultramicropores (as in the case of zeolites): in fact the strong adsorbate–pore wall interaction and the low (pore size/adsorbate molecular size) ratio makes the adsorption very different from that observed on open surfaces (a straight line is not obtained on these solids).

If the solid contains mesopores [3,34] an upward deviation from the linearity corresponding to the capillary condensation is observed. After the complete filling of mesopores a new straight line with a slope correspondent to the lower external surface area is obtained. The intercept of this line with ordinate gives the mesopore and, if present, micropore volume; unfortunately in most cases the straight part is too short to allow the calculation.

As shown, the method, beside surface area, allows the calculation of micropore and/or mesopore volume or, more exactly, of the volume V_{f} of gaseous nitrogen necessary to fill the pores. To calculate the physical volume of pores V_{p} it is necessary to know the density of the adsorbate inside the pores. According to the so-called Gurvitsch rule (see Section 3.9), the adsorbate density is generally close to the liquid density *pl* at the measurement temperature [3,35] even for microporous solids, so that pore volume is given by

$$V_p = (V_f/22414)M/pl.$$

Nowadays t-plot is the best method to calculate total micropore volume. The success of the method depends on the choice of the reference isotherm (isotherm used to determine the dependence of t vs. p/p_s). In the first monolayer formation range sharpness of the isotherm depends on the adsorbate–surface interaction, represented by parameter c in BET equation. Obviously a reference isotherm suitable for all solids does not exist. Many isotherms have been proposed as reference for different classes of solids (oxides, activated carbons and so on) in many cases obtained by adsorption on similar nonporous compounds, and in other cases semi-empirical equations have been developed [3,29,30,36–39]. The mathematical form of the most common reference isotherm is [21,40,41]:

$$t = 3.54(5/\ln p/p_s)^{1/3} \quad \text{(Halsey)}$$

$$t = (13.99/(0.034 - \log p/p_s))^{1/2} \quad \text{(Harkins–Jura)}$$

$$t = 3.7(5/\ln p/p_s)^{1/3} + p/p_s^{1/2} - 0.8 \quad \text{(Cranston–Inkley)}$$

By changing the reference isotherm both slope and intercept with the ordinate (i.e. surface area and pore volume) change. The best choice is a reference isotherm obtained on a solid similar to that under study. Alternatively it is necessary to use a proper equation (generally available in the software of commercial instruments; see the above reported examples), but in this case comparison with results of independent methods is highly recommended and modification of some parameter of the equation can be necessary.

3.3. α_s-plot method (surface area, micropore and mesopore volume)

The method, a variant of t-plot method, has been proposed by Sing in 1969 [3,31,42,43] and is still widely used (see for example papers collected in [7,8]).

The starting point is the observation that what t-plot method really do is to compare the shape of isotherm under test with that of a standard isotherm. Under this point of view it is enough to normalize the adsorption at a given value of p/p_s. So the method uses the quantity α_s, that is the ratio between the adsorbed volume and the adsorbed volume at p/p_{s}=0.4. The surface area of the sample under test can be directly calculated from the surface area of the reference material by the simple relation:

$$A_s = A_s(\text{reference})V_{\text{ads}}\,(\text{sample at}\,p/p_s\,0.4)/ V_{\text{ads}}(\text{reference at}\,p/p_s 0.4)$$

The pore volume can be calculated as in the *t*-plot method.

An extension of the method to very low p/p_s region (high resolution as-plot) has been used, with some interesting results, to investigate micropores [2,44].

3.4. DR-plot (micropore volume)

This is the early method proposed for micropore volume determination [45,46]. Although still used [47]; see also [7,8], it has been progressively neglected, because its validity has been questioned both from theoretical stand point and practical unsuccess in its application [3,48,49].

3.5. MP method (micropore volume and micropore size distribution)

It is a matter of a method derived from *t*-plot with the aim to calculate the pore size distribution of microporous (but not ultramicroporous) solids such as active carbons [33]. Comments are the same as those above reported for DR-plot method.

3.6. Horvath–Kavazoe method (micropore volume and micropore size distribution)

The method, developed for parallel plates shaped pores (for instance present in many active carbons), is based on a quasi-thermodynamic approach: the average potential function inside the pores is calculated relating the average interaction energy of an adsorbed molecule to its free energy change under adsorption [50]. The result is a complex equation in which pore size is related to the relative pressure at which the pore is filled by the adsorbate. For cylindrical pores (for example zeolite cavities) a variant has been proposed by Saito and Foley [51].

The method, ignored for a few years, has been used since the end of 1980s and is now available in the software of some commercial instruments. However, the method shows some defects. Particularly the adsorption process is described as a sudden and complete filling of empty pores, instead of the result of a progressive adsorption. Thus the model calculates the adsorption in partially filled pores and on external surfaces as the filling of new pores.

The results can be used, with caution, in the case of active carbons, but are unsatisfactory in the case of ultramicroporous solids, for example zeolites: the progressive filling of channels is interpreted as a nonuniform pore size distribution.

The method is not applicable to pores larger than 1.5 nm [50].

3.7. DFT methods (pore volume and pore size distribution)

The methods based on density functional theory (DFT) represent the more recent approach to the calculation of pore volume and pore size distribution (particularly for micropores) from adsorption isotherm. DFT has been first used by Seaton and coworkers [52] and successively has been improved mainly by researchers of the same group [53,54] and by Olivier and Conklin [55,56]. The approach consists of the construction of a grand potential functional of the average local density and of a minimization of this with respect to local density to obtain equilibrium density profile and thermodynamic properties. The proposed approaches differ according to the smoothed density approximation term used.

The method has no theoretical limitations as the pore size is concerned: in practice its applicability ranges from ultramicropores to macropores, with the lower size limitation due to the adsorbate molecular size and the upper size limitation arising from the difficulty to perform precise measurements near saturation.

Although the method is not yet settled, very promising results are being obtained, also for microporous solids and commercial software becomes to be available. People working on microporous solids should try to use this method to check its suitability to their material.

3.8. BJH method (mesopore volume and mesopore size distribution)

Many methods, based on Kelvin equation, have been developed to describe the adsorption-capillary condensation process that takes place in mesopores. We can quote the methods proposed by Barrer, Joiyner and Halenda (BJH method) [57], Pierce [58], Orr and Dalla Valle [59], Shull [29], Dubinin [60], Cranston and Inkley [30], Dollimore and Heal [61], Brokeoff and DeBoer (“modelless” method; [62]), Klinik and Jagello [60] and so on.

Although each method has both advantages and disadvantages, the BJH method is the most widely used: it is designed as ASTM standard method D 4641/87 and is widely used also by commercial instruments to perform calculation on mesopores.

The model is simple [2,3,21]. In the capillary condensation region (p/p_s>0.4), each pressure increase causes an increase of the thickness of layer adsorbed on pore walls (as foreseen by t-plot model) and capillary condensation in pores having a core (i.e. the empty space of pores) size r_c defined by Kelvin equation:

$$\ln(p/p_s) = -(2\gamma w_m \cos\theta)/(RTr_c),$$

where r_c represents the radius for cylindrical pores, the distance between walls for slit shaped pores γ, the surface tension, w_m the molar volume and θ the contact angle.

The assumption of a geometric model (usually cylindrical or slit shaped) allows the calculation of the contribution of the thickness of the adsorbed film to the total adsorption and then the core volume. From these results and from the assumed pore geometry it is possible to transform the core volume into the pore volume and the core size into the pore size.

In such a way, by examining step by step the isotherm in the range $0.42<p/p_s<0.98$, the mesopore volume and the mesopore size distribution can be obtained.

The lower limit is probably due to the tensile strength effect [3,63], even if the problem is still open [4]. The maximum tension that a liquid can withstand is equal to its tensile strength. Since the tension increases as p/p_s decreases, there is a minimum value of p/p_s (then of pore size) at which the liquid condensed in the pores can exist. For the same reason the hysteresis loop closure takes place always at 0.42, using nitrogen as adsorbate.

The upper limit has no theoretical reasons [3]. The limitation arises from the exponential dependence of pore size in which the condensation takes place from the relative pressure. Thus, errors in pressure measurements have an increasing effect as the pressure approaches the saturation value. Moreover, the effect of uncertainty in the temperature of the sample becomes progressively larger as $p/p_s \rightarrow 1$.

Since the method gives the distribution of pore volume against the pore size, the choice of a geometric model for the pores allows the calculation of the surface area (the surface of mesopore walls) as a function of pore size [3,57,60]. Unfortunately, the necessity to assume a geometric model affects the obtained surface data more strongly than in the case of pore volume and the results require independent confirmations, for example by comparing them with those obtained by applying t-plot method (surface area external to micropores), mercury porosimetry and so on.

3.9. Gurvitsch volume method (micropore plus mesopore volume)

The high pressure plateau observed in the case of solids containing mesopores (type IV isotherm) corresponds to the complete filling of meso and (if present) micropores. In quite all the cases the adsorbate density corresponds to the liquid density at measurement temperature as indicated by the so-called Gurvitsch rule: using the liquid density the same volume is obtained independent of the adsorbate [3,35]. This allows a simple (and independent of pore geometry) model to estimate the pore volume from the quantity of adsorbate correspondent to the flex point of the high pressure plateau. The method is useful to verify the reliability of results obtained by other methods.

4. Kripton, argon and helium adsorption at low temperature (surface area and micropore volume)

Noble gases, having spherical nonpolar molecules, can give some valid alternatives to nitrogen, at least in special cases.

Kr and Ar adsorption at 77 K can be advantageously used to determine low (<1 m^2g^{-1}) surface area (see [3] and references therein, and [21]). Ar adsorption at 77 and 87 K [64,65] and He adsorption at 4.2 K [2,66,67] have been used to investigate microporous solids.

5. Mercury porosimetry (meso and macropore volume and size distribution)

Since the contact angle of mercury with most solids is higher than 90°, it penetrates pores only when forced by pressure, following the Washburn equation [2,3,68]:

$$P = (2\gamma\cos\theta)/r_\mathrm{p},$$

where P is the applied pressure, γ the surface tension, θ the contact angle and r_p the pore size (i.e. the radius for cylindrical pores, the distance between walls for slit shaped ones). The measurement range offered by commercial instruments is 1–2000 atm, corresponding to 7.5–15 000 nm.

The behaviour is opposite to that of nitrogen (having a contact angle <90°). As the pressure increases mercury fills progressively finer pores: a plot of intruded mercury volume (that is the pore volume) against pore size is obtained.

Since θ is not easy to measure, a value of 140° is generally used, independent of the solid under test [3,68,69]. The value of pure mercury must be assumed for γ, even if it is sensitive to contamination from the solid [3,68]. Uncertainty in θ and γ causes an overall error difficult to assess: quantitatively it can vary from negligible to very large. So a comparison with results obtained with other techniques is highly recommended whenever is possible (Fig. 6).

In the case of a nonuniform pore (for example ink-bottle shaped) the pore size corresponds to that of pore mouth. Since in most solids a porous network is present, the interpretation of results is affected by pore blocking effects [70,71].

Working under pressure requires some care because it can cause compression of soft solids or breakage of pore walls. This is the case of very high porous silica obtained by sol–gel method [72–74]. As for nitrogen adsorption, mercury porosimetry shows a hysteresis loop, which is difficult to interpret and the information obtained is rather questionable, at least in our opinion. For more details see [3,70,71,75].

Despite its limitations, mercury porosimetry, designed as ASTM standard method D 4284/83 remains a fundamental technique to study macropores up to 15 000 nm, otherwise not possible with techniques based on vapour adsorption. In the mesopore range both techniques can be used and the results are often in good agreement ([3,76,77] Fig. 6).

If some disagreement is observed, it probably arises by nonappropriate choice of the pore, of the value of θ or γ, or of the reference curve for the thickness of nitrogen adsorbed layer.

6. Incipient wetness method (total pore volume)

Following this method [78,79], the solid is impregnated with a nonsolvent liquid, usually water or hydrocarbons, necessary to fill the pores completely. Addition of liquid must be stopped when the solid tends to become sticky or if a large excess has been used, the liquid can be removed by centrifugation. In that condition the pore volume is equal to the volume of the liquid adsorbed by the solid.

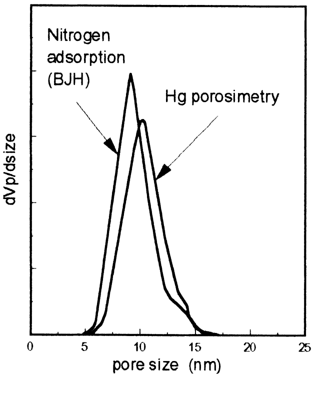

Method	Vp (cm3/g)	Pore size (nm)
N2 (BJH)	0.48	9.5
N2 (Gurvitsch)	0.50	-
Hg porosimetry	0.46	10.5
Inc. wetness	0.52	-

Fig. 6. Comparison among different methods for mesopore volume and size calculation

This is a good, precise method, very useful to validate results obtained with other techniques. By the way, it is the only one that can be applied on high porous silica.

7. Picnometry (total pore volume)

True density p_t (i.e. the chemical density corrected for the contribution of possible blind pores) and particle density p_p (i.e. the chemical density corrected for the contribution of all the pores) allow the calculation of total pore volume from the equation [9]:

$$V_p = p_p^{-1} - p_t^{-1}.$$

Both densities can be measured by the usual picnometry, p_t with He picnometry and p_p with mercury picnometry [9]. He penetrates all the cavities while mercury only pores smaller than 15 000 nm at atmospheric pressure. Then this simple method is suitable for all the solids with pores no larger than 15 000 nm and can be used to confirm results from other techniques.

8. Permeametry and counterdiffusion (average diffusive pore size and tortuosity factor)

Up to now all the efforts to utilize directly the pore size distribution, obtained with the above described techniques, interpreting quantitatively mass transfer processes inside the pores have failed. Permeametry and counterdiffusion allow to obtain the values of "average diffusive diameter" and "tortuosity factor" that are directly used in equations describing mass transfer in catalyst pores [9,80,81].

Both techniques require the gas to flow only through the pores of a shaped catalyst fixed to a nonporous support. In permeametry a slight pressure difference between the two faces of the catalyst particles is established and the equilibration pressure rate is recorded. Counterdiffusion, known also as Wicke–Kallenbach technique, measures the diffusional counterflux of two gases of different molecular weight through catalyst particles. Suitable models allow to calculate the desired parameters. All apparatus are laboratory made.

9. Other methods

Many other methods have been proposed to study surface area and pore structure of solids. They are less widely used than those reported in previous sections because of various reasons. In some cases they require more expensive instruments or techniques generally managed in specialistic laboratories. In other cases there are strong limitations to their use. Finally the physical meaning of the result can be rather uncertain.

Nevertheless in the following they are listed for sake of completeness:

1. Small angle X-ray and neutron scattering [1,2,7(three papers), 8(five papers), 82]
2. NMR and Xenon NMR [1,83–85],
3. Thermoporometry [1,2,84,86],
4. Calorimetry [1,3,18,20],
5. Electron microscopy [1,2,87–89],
6. Molecular sieve method [50].

10. Choice of the methods

On the basis of our experience, the methods that give the best results are:

1. total surface area: BET method,
2. surface area external to micropores: *t*-plot, a_s-plot methods,
3. total pore volume: incipient wetness method, picnometry, Gurvitsch method (if applicable),
4. total micropore volume: *t*-plot, a_s-plot methods,
5. total micropore and mesopore volume: Gurvitsch volume method,
6. mesopore volume and mesopore size distribution: BJH method, mercury porosimetry,
7. macropore volume and macropore size distribution: mercury porosimetry.

The other quantities do not make sense (micropore surface area) or the results can be questionable and require independent confirmations (micropore size distribution, mesopore surface area, macropore surface area). DFT method deserves a special mention: although not yet completely assessed, it appears very promising, offering the possibility to obtain a complete micro and mesopore size distribution.

References

[1] J. Roquerol et al., in: J. Roquerol et al. (Eds.), Characterization of Porous Solids III, Elsevier, Amsterdam, 1994, p. 1.
[2] K. Kaneko, J. Membr. Sci. 96 (1994) 59.
[3] S.J. Gregg, K.S.W. Sing, Adsorption, Surface Area and Porosity, Academic Press, London, 1982.
[4] D.H. Everett, in: K.K. Unger et al. (Eds.), Characterization of Porous Solids, Elsevier, Amsterdam, 1988, p.1.
[5] K.W. Sing, in: F. Rodrguez-Reinoso et al. (Eds.), Characterization of Porous Solids II, Elsevier, Amsterdam, 1991, p.1.
[6] K.K. Unger, J. Roquerol, K.S.W. Sing, H. Kral (Eds.), Characterization of Porous Solids, Elsevier, Amsterdam, 1988.
[7] F. Rodriguez-Reinoso, J. Roquerol, K.S.W. Sing, K.K. Unger (Eds.), Characterization of Porous Solids II, Elsevier, Amsterdam, 1991.
[8] J. Roquerol, F. Rodriguez-Reinoso, K.S.W. Sing, K.K. Unger (Eds.), Characterization of Porous Solids III, Elsevier, Amsterdam, 1994.
[9] J.T. Richardson, Principles of Catalyst Development, Plenum Press, New York, 1989.
[10] D. Sanfilippo (Ed.), The Catalytic Process from Laboratory to the Industrial Plant, Proceedings of the Third Seminar of Catalysis, Rimini, 1994.
[11] K.S.W. Sing et al., Pure Appl. Chem. 57 (1985) 603.
[12] R.M. Barrer et al., J. Colloid Interface Sci. (1956) 479.
[13] L.H. Cohan, J. Am. Chem. Soc. 66 (1944) 98.
[14] J.H. DeBoer, The Structure and Properties of Porous Materials, Butterworths, London, 1958.
[15] M.R. Barrer, D.M. McLeod, Trans. Fararaday Soc. 50 (1954) 980.
[16] S. Brunauer, P.H. Emmet, J. Am. Chem. Soc. 60 (1938) 309.
[17] S. Brunauer, The Adsorption of Gases and Vapors, University Press, Oxford, 1945.
[18] W.D. Harkins, G. Jura, J. Am. Chem. Soc. 66 (1944) 1362.
[19] R.T. Davis, T.W. DeWitt, J. Phys. Chem. 51 (1947) 1232.
[20] S. Partyka, F. Roquerol, J. Roquerol, J. Colloid Interface Sci. 68 (1979) 21.
[21] D.M. Young, A.D. Crowell, Physical Adsorption of Gases, Butterworths, London, 1962.
[22] D.L. Kantro, S. Brunauer, L.E. Copeland, in: E.A. Flood (Ed.), The Solid–Gas Interface, Chapters 3, 12, Marcel Dekker, New York, 1967 .
[23] G. Leofanti, Unpublished results.
[24] T.L. Hill, J. Chem. Phys. 14 (1946) 263.
[25] W.A. Steele; The Interaction of Gases with Solid Surfaces, Pergamon Press, Oxford, 1974.
[26] G.D. Halsey, J. Chem. Phys. 16 (1948) 931.
[27] R.M. Barrer, N. MacKenzie, D. McLeod, J. Chem. Soc. (1952) 1736.
[28] B.C. Lippens, J.H. DeBoer, J. Catal. 4 (1965) 319.
[29] C.G. Shull, J. Am. Chem. Soc. 70, (1948) 1405.
[30] R.W. Cranston, F.A. Inkley, Adv. Catal. 9 (1957) 143.
[31] K.S.W. Sing, in: D.H. Everett, R.H. Ottewill (Eds.), Surface Area Determination, Butterworths, London, 1970.
[32] M. Jeziorowski, H. Knozinger, W. Meye, J. Colloid Interface Sci. 50 (1975) 283.
[33] R.Sh. Mikhail, S. Brunauer, E.E. Bodor, J. Colloid Interface Sci. 26 (1968) 45,54.
[34] G. Leofanti, Unpublished results.
[35] D. Dollimore, T. Shingles, J. Appl. Chem. 19 (1969) 218.
[36] M.R. Brambhani, P.A. Cutting, K.S.W. Sing, D.H. Turk, J. Colloid Interface Sci. 38 (1972) 109.
[37] J.H. DeBoer, in: D.H. Everett, R.H. Ottewill (Eds.), Surface Area Determination, Butterworths, London, 1970.
[38] S. Brunauer, R.S. Mikhail, E.E. Bodor, J. Colloid Interface Sci. 24 (1967) 451.
[39] A. Lecloux, J.P Pirad, J. Colloid Interface Sci. 70 (1979) 265.
[40] B.G. Linsen, A. van den Heuvel, in: E.A. Flood (Ed.), The Solid–Gas Interface, Chapter 35, Marcel Dekker, New York, 1967 .
[41] User's manuals of commercial instruments.
[42] D. Atkinson, A.I. McLeod, K.S.W. Sing, J. Chim. Phys. 81 (1984) 791.
[43] K.S.W. Sing, Carbon 30 (1992) 1075.
[44] K. Kaneko, C. Ishii, Colloid Surf. 67 (1992) (203).
[45] M.M. Dubinin, L.V. Radushkevich, Proc. Acad. Sci USSR 55 (1947) 331.
[46] M.M. Dubinin, V.A. Astakhov, Adv. Chem. Ser. 102 (1971) 69.
[47] M.M. Dubinin, H.F. Stoeckli, J. Colloid Interface Sci. 75 (1980) 34.
[48] H. Marsh, B. Rand, proceedings of the Third Conference on Industrial Carbon and Graphite, Academic Press, London, 1970, p. 93.
[49] J.A. Lee, C.E. Newnham, J. Colloid Interface Sci. 56 (1976) 391.
[50] G. Horvath, K. Kavazoe, J. Chem. Eng. Jap. 16 (1983) 470.
[51] A. Saito, H.C. Foley, AIChE J. 37 (1991) 429.
[52] N.A. Seaton, J.P.R.B. Walton, N. Quirke, Carbon 27 (1989) 853.
[53] C. Lastoskie, K.E. Gubbins, N. Quirke, in: Proceedings of the International Symposium on Effects of Surface Eterogeneity in Adsorption and Catalysis on Solids, Kazimierz Dolny, Poland, 1992.
[54] C. Lastoskie, K.E. Gubbins, N. Quirke, in: J. Roquerol et al. (Eds.), Characterization of Porous Solids III, Elsevier, Amsterdam, 1994, p. 51.
[55] J.P. Olivier, W.B. Conklin, in: Proceedings of the International Symposiun on Effects of Surface Eterogeneity in Adsorption and Catalysis on Solids, Kazimierz Dolny, Poland, 1992.
[56] J.P. Olivier, W.B. Conklin, in: J. Roquerol et al. (Eds.), Characterization of Porous Solids III, Elsevier, Amsterdam, 1994, p. 51.
[57] E.P. Barret, L.G. Joiyner, P.P. Halenda, J. Am. Chem. Soc. 73 (1953) 373.
[58] C. Pierce, J. Phys. Chem. 57 (1953) 149.
[59] C. Orr, J.M. Dalla Valle, Fine Particle Measurement, Macmillan, New York, 1959, p. 271.
[60] J. Klinik, in: J. Roquerol et al. (Eds.), Characterization of Porous Solids III, Elsevier, Amsterdam, 1994, p. 119.

[61] D. Dollimore, G.R. Heal, J. Appl. Chem. 14 (1964) 109.

[62] J.P.C. Brokeoff, J.H. DeBoer, J. Catal. 9 (1967) 9, 15; 10 (1968) 368, 377, 391.

[63] O. Kadlec, M.M. Dubinin, J. Colloid Interface Sci. 31 (1969) 479.

[64] S.W. Webb, W.C. Cconner, in: F. Rodriguez-Reinoso et al. (Eds.), Characterization of Porous Solids II, Elsevier, Amsterdam, 1991, p. 31.

[65] H. Reichert et al. in: F. Rodriguez-Reinoso et al. (Eds.), Characterization of Porous Solids II, Elsevier, Amsterdam, 1991, p. 535.

[66] N. Setoyama et al., Langmuir 9 (1993) 2612.

[67] W.A. Steele, J. Chem. Phys. 25 (1959) 919.

[68] H.L. Ritter, L.C. Drake, Ind. Eng. Chem. Analyt. Ed. 17 (1945) 782.

[69] S. Lowell, Powder Technol. 37 (1980) 37.

[70] M. Day et al., in: J. Roquerol et al. (Eds.), Characterization of Porous Solids III, Elsevier, Amsterdam, 1994, p. 225.

[71] R. Mann, G.P. Androutsopoulos, H. Golshan, Chem. Eng. Sci. 36 (1981) 337.

[72] R. Sibut Pinote, P. Cournnault, F. Du Chaffant, J. Chim. Phys. 65 (1968) 1188.

[73] J.M. Dickinson, J.W. Shore, Carbon 6 (1968) 937.

[74] S.M. Brown, E.W. Lard, Powder Technol. 9 (1974) 187.

[75] W.C. Conner, A.M. Lane, A.J. Hoffmann, J. Colloid Interface Sci. 100 (1984) 185.

[76] B.D. Adkins, J.B. Heink, B.H. Davis, Adsorpt. Sci. Technol. 4 (1987) 87.

[77] B.D. Adkins, B.H. Davis, Adsorpt. Sci. Technol. 5(76) (1988) 168.

[78] W.B. Innes, Anal. Chem. 23 (1951) 759.

[79] M.P. MsDaniel, T.D. Hottovy, J. Colloid Interface Sci. 78 (1980) 31.

[80] C.N. Satterfield, Mass Transfer in Heterogeneous Catalysis, MIT Press, Cambridge, 1970.

[81] J. Valus, P. Schneider, Appl. Catal. (1985) 329.

[82] A.J. Renouprez, in: B. Imelik, J.C. Vedrine (Eds.), Catalyst Characterization, Plenum Press, New York, 1988, p.445.

[83] Y. Ben Taarit, J. Fraissard, in: B. Imelik, J.C. Vedrine (Eds.), Catalyst Characterization, Plenum Press, New York, 1988, p. 91.

[84] D.M. Smith, P.J. Davis, in: F. Rodrguez-Reinoso et al. (Eds.), Characterization of Porous Solids II, Elsevier, Amsterdam, 1991.

[85] W.L. Earl, Y.W. Kim, D.M. Smith, in: J. Roquerol et al. (Eds.), Characterization of Porous Solids III, Elsevier, Amsterdam, vol. 87, 1994, p. 301.

[86] M. Pauthe, J.F. Quinson, J.D.F. Ramsay, in: J. Roquerol et al. (Eds.), Characterization of Porous Solids III, Elsevier, Amsterdam, 1994, p. 283.

[87] H. Dexpert, P. Gallezot, C. Leclercq, in: B. Imelik, J.C. Vedrine (Eds.), Catalyst Characterization, Plenum Press, New York, 1988, p. 509.

[88] R.W. Innes, J.R. Fryer, H.F. Stoeckli, Carbon 14 (1976) 7.

[89] B. McEnaney, T.J. Mays, in: J. Roquerol et al. (Eds.), Characterization of Porous Solids III, Elsevier, Amsterdam, 1994, p. 327.